J. Ocean Univ. China (Oceanic and Coastal Sea Research)
https://doi.org/10.1007/s11802-018-3452-7
ISSN 1672-5182, 2018 17 (1): 169-176
http://www.ouc.edu.cn/xbywb/
E-mail:xbywb@ouc.edu.cn

Seismogenic Structures of the 2006 M_L4.0 Dangan Island Earthquake Offshore Hong Kong

XIA Shaohong[1), *], CAO Jinghe[1)], SUN Jinlong[1)], LV Jinshui[2)], XU Huilong[1)], ZHANG Xiang[1), 2), 3)], WAN Kuiyuan[1), 3)], FAN Chaoyan[1), 3)], and ZHOU Pengxiang[1), 3)]

1) *CAS Key Laboratory of Ocean and Marginal Sea Geology*, *South China Sea Institute of Oceanology*, *Chinese Academy of Sciences*, *Guangzhou* 510301, *China*
2) *Seismological Bureau of Guangdong Province*, *Guangzhou* 510070, *China*
3) *University of Chinese Academy of Sciences*, *Beijing* 100049, *China*

(Received February 23, 2017; revised August 5, 2017; accepted September 27, 2017)

Abstract The northern margin of the South China Sea, as a typical extensional continental margin, has relatively strong intraplate seismicity. Compared with the active zones of Nanao Island, Yangjiang, and Heyuan, seismicity in the Pearl River Estuary is relatively low. However, a M_L4.0 earthquake in 2006 occurred near Dangan Island (DI) offshore Hong Kong, and this site was adjacent to the source of the historical M5.8 earthquake in 1874. To reveal the seismogenic mechanism of intraplate earthquakes in DI, we systematically analyzed the structural characteristics in the source area of the 2006 DI earthquake using integrated 24-channel seismic profiles, onshore–offshore wide-angle seismic tomography, and natural earthquake parameters. We ascertained the locations of NW- and NE-trending faults in the DI sea and found that the NE-trending DI fault mainly dipped southeast at a high angle and cut through the crust with an obvious low-velocity anomaly. The NW-trending fault dipped southwest with a similar high angle. The 2006 DI earthquake was adjacent to the intersection of the NE- and NW-trending faults, which suggested that the intersection of the two faults with different strikes could provide a favorable condition for the generation and triggering of intraplate earthquakes. Crustal velocity model showed that the high-velocity anomaly was imaged in the west of DI, but a distinct entity with low-velocity anomaly in the upper crust and high-velocity anomaly in the lower crust was found in the south of DI. Both the 1874 and 2006 DI earthquakes occurred along the edge of the distinct entity. Two vertical cross-sections nearly perpendicular to the strikes of the intersecting faults revealed good spatial correlations between the 2006 DI earthquake and the low to high speed transition in the distinct entity. This result indicated that the transitional zone might be a weakly structural body that can store strain energy and release it as a brittle failure, resulting in an earthquake-prone area.

Key words Dangan Island; intraplate seismicity; South China Sea; crustal velocity model; seismogenic structure

1 Introduction

Over 90% of the world's earthquakes occur at the edge of oceanic and continental plates (Rocha *et al*., 2016). Unlike plate boundary regions where seismicity is relatively concentrated and has become increasingly well understood (Zoback, 2010), the causes of intraplate seismicity in stable continental interiors are still a challenge in seismology (Assumpcao *et al*., 2004). Intraplate seismicity reflects diffuse deformation in relatively stable tectonic regions (Zoback, 1992). Their origins are closely associated with the reactivation of pre-existing zones of weakness (Sykes, 1978), such as extended crust in aborted rifts or continental margins (*e.g.*, Talwani, 1988; Schulte and Mooney, 2005) or stress concentration in the upper crust due to structural inhomogeneities (*e.g.*, Sykes, 1978; Talwani, 1988; Talwani and Rajendran, 1991; Kenner and Segall, 2000). In addition, lithospheric thinning also provides favorable conditions for stress concentration in the brittle upper crust (Assumpcao *et al*., 2004).

The northern margin of the South China Sea (SCS) is an extensional continental margin, but it is also considered an intraplate region with moderate to high seismic activity levels. A large number of NE-, NEE-, NW-, and EW-trending faults are widely distributed in the coastal region of the northern SCS (Fig.1). According to the monitoring data of seismic network in the past 10 years, strong seismicity is mainly concentrated in Nanao Island, Yangjiang, and Heyuan (Fig.2), whereas seismicity is relatively low in the Pearl River Estuary. The distribution of historically large earthquakes with magnitude larger than M6.0 also indicates that seismic activity levels ap-

* Corresponding author. Tel: 0086-20-89107065
E-mail: shxia@scsio.ac.cn

pear to be significantly lower in the Pearl River Estuary (including Hong Kong, Shenzhen, Guangzhou, and Macau) than in the eastern and western coastal regions of the northern SCS (Chandler and Lam, 2002). Almost all highly destructive earthquakes with magnitude greater than 7.0 in historic times occurred along the NE-trending littoral fault zone (LFZ) nearly parallel to the coastline. As a part of the LFZ, the Dangan Island (DI) fault, which lies about 30 km southeast of Hong Kong and has generated two moderate earthquakes in 1874 (about M5.8) and 2006 (M_L4.0), may produce earthquakes with magnitude of 7.0 (Chau *et al*., 2004). The results of ground motion simulations revealed that strong earthquakes with M6.0–6.5 along the DI fault, rather than major distant earthquakes, would dominate the seismic hazard and cause severe building damage in Hong Kong (Megawati, 2007). Therefore, a detailed seismogenic structure in the DI sea area must be obtained.

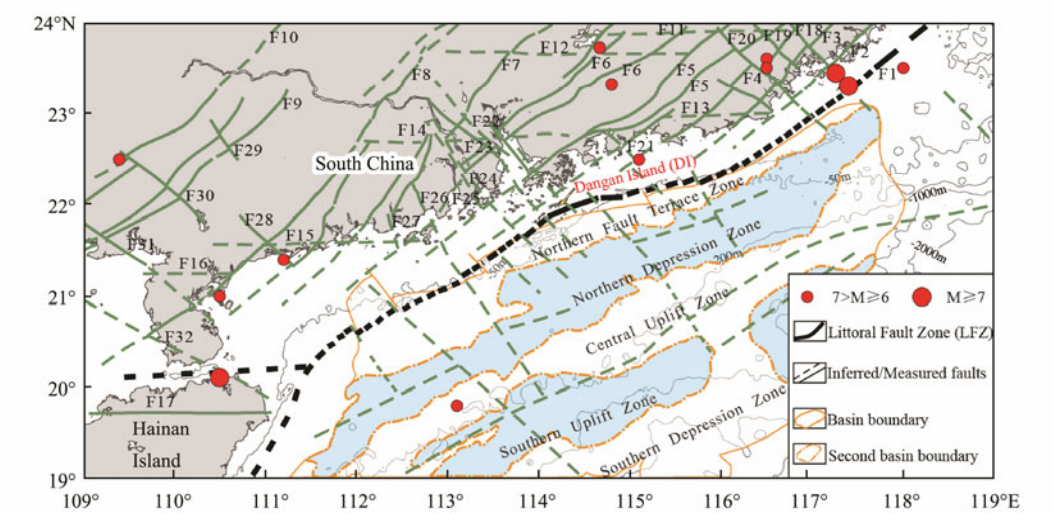

Fig.1 Distribution of faults with different strikes in the coastal region of Guangdong. Locations of most faults on the sea could be inferred. The red circles denote the earthquakes with magnitude larger than M6.0. Earthquakes with magnitude greater than M7.0 mainly occurred along the Littoral Fault Zone (LFZ).

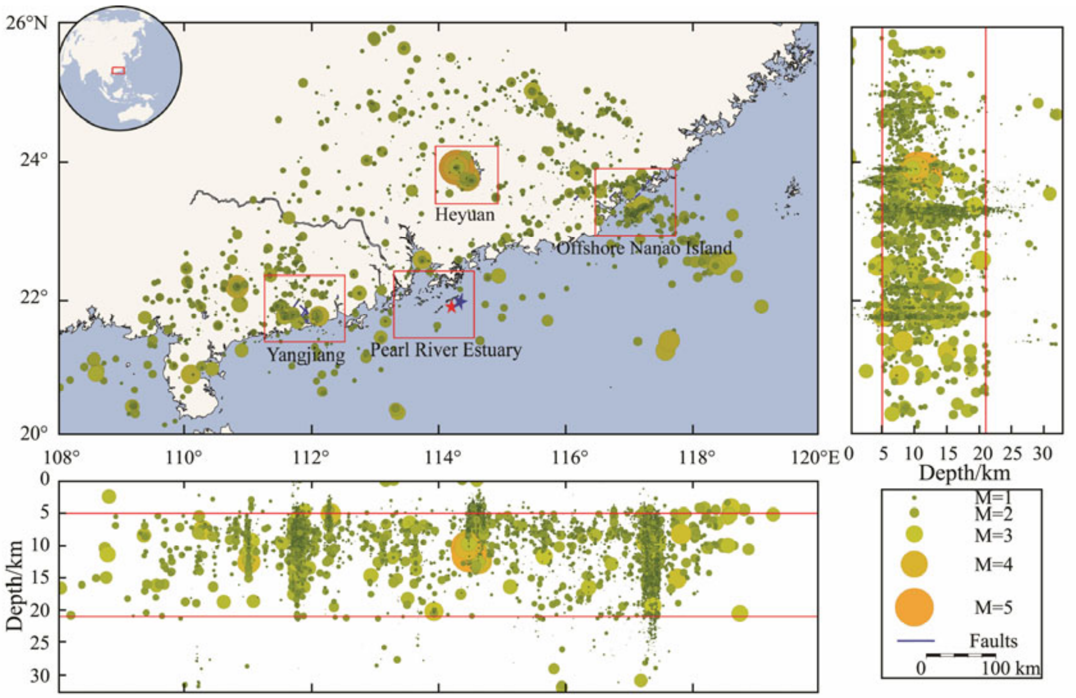

Fig.2 Distribution of seismicity in the coastal region of Guangdong from the last ten years of the seismic network in Guangdong. The focal depth of earthquakes was mainly located at 5–20 km. The seismicities of Yangjiang, Heyuan, and offshore Nanao Island areas are strong. The seismicity in the Pearl River Estuary is relatively low, but two earthquakes with M5.8 in 1874 (blue star) and M4.0 in 2006 (red star) occurred near Dangan Island, called Dangan Island earthquakes.

Given the poor correlation between intraplate seismicity and surface geological patterns, seismic investigations have become one of the most useful tools to understand the mechanisms of earthquakes in intraplate tectonic settings (*e.g.*, Hole *et al*., 2001; Assumpcao *et al*., 2004; Kato *et al*., 2009). Results from seismic velocity models implied the important roles of fluids (Reyners *et al*., 2007), lithosphere/asthenosphere topography (Assumpcao *et al*., 2004), and ancient rift systems (Kato *et al*., 2009) in intraplate seismicity, and such findings revealed the location of the faults (*e.g.*, Wittlinger *et al*., 1998; Hole *et al*., 2001). Intraplate seismicity generally occurs in the vicinity of stress concentrators within pre-existing zones of weakness, including intersecting faults, buried plutons, and rift pillows (Gangopadhyay and Talwani, 2003), which is consistent with the tomographic results that intraplate earthquakes occur in the transition zones between high and low velocities (Koulakov *et al*., 2010).

Most previous studies on seismic investigations focused either onshore or at sea only in the northern margin of the SCS (*e.g.*, Nissen *et al*., 1995; Qiu *et al*., 2001; Zhang and Wang, 2007), and their main purposes were to study deep crustal structures, tectonic features of rifting continental margin, and formation and evolution of sedimentary basins. Although the latest seismic surveys in the onshore–offshore transitional zone of the northern SCS have been implemented and yielded new findings (*e.g.*, Xia *et al*., 2010, 2012; Zhao *et al*., 2004a; Cao *et al*., 2014), these studies have been limited to image crustal velocity models, infer the location of the LFZ, and reveal variations in crustal structures. The seismogenic structure and spatial variability of faults remain largely ignored. Thus, this study aimed to use integrated seismic data to ascertain the location of the intersection of different strike faults, systematically analyze the structural variations in the source area, and reveal the seismogenic structures of the 2006 DI earthquake.

2 Tectonic Setting

The SCS is one of the biggest marginal seas of the western Pacific, and it has experienced continental rifting, breakup, subsequent seafloor spreading, and current subduction of the oceanic crust (Taylor and Hayes, 1983; Tapponnier *et al*., 1986; Li *et al*., 2012; Sibuet *et al*., 2016). Considering the complicated interaction among the Pacific Plate in the east, the Eurasian Plate in the north, and the Indian–Australian Plate in the west and south, the formation and evolution of the SCS have always been the focus of attention of geologists at home and abroad (*e.g.*, Briais *et al*., 1993; Lester *et al*., 2014; Li *et al*., 2015; Sibuet *et al*., 2016). The northern margin is the only well-preserved extensional margin of the SCS (Gao *et al*., 2016), and it has an important tectonic position. It not only records important information about the rifting evolution process and tectonic features of the SCS (Xia *et al*., 2010; Barckhausen *et al*., 2014), but it is also the significant cohesive zone from the convergent margin in late Mesozoic to the rifting margin in Cenozoic (Li and Li, 2007; Shi and Li, 2012). Intrusion of magma and igneous rocks extensively occurs in the northern margin of the SCS (Yan *et al*., 2001; Wang *et al*., 2006). Under the comprehensive influences of the NW-ward subducting Philippines Sea plate and the extrusion of the Indo–Tibet collision, neotectonic movement in the northern margin is very strong (Liu, 1981), which is characterized by strong seismic activity, fault movement, tectonic uplift, and sea level changes. Since the earliest historical records, 11 earthquakes with magnitude larger than M6.0 have occurred in the coastal region, including four earthquakes with magnitude larger than M7.0 that belong to the typical intraplate seismic belt. These large earthquakes are characterized by shallow focal depth and strong destructiveness, causing serious loss of life and property.

Structurally, the northern margin of the SCS is characterized by an intersecting network with different strike faults (Fig.1), which include dominant NE-trending set, NEE–E-trending set, and subordinate NW-trending set (Pigott and Ru, 1994; Liu *et al*., 1997). These fault sets have had an important and long-lived influence on magmatism and tectonics with individual faults acting as conduits for magmas and the loci of fissure-like volcanic centers (Ding and Lai, 1997; Campbell and Sewell, 1997). The main performance of NE-trending faults is large scale, extending up to several hundred kilometers or even thousands of kilometers. This set of faults is characterized with deep dissection, large separation, and major width of the section. Strong metamorphism, such as extensive schist and gneiss, siliceous rock, and mixed rock along the faults, is composed of huge metamorphic belts. The NE-striking elongated calderas, delineated by ring faults and ring-like intrusions, indicate strong control of NE-trending faults on the distribution and loci of volcanic centers (Ding and Lai, 1997; Campbell and Sewell, 1997). The NW-trending faults are relatively small scale, show intermittent distribution of shadows, and extend thousands of meters to dozens of meters, with the largest up to hundreds of kilometers. This set of faults was active during the middle Jurassic to early Cretaceous volcanism (Campbell and Sewell, 1997) and has also been the focus of some recent fault activity (Lee and Workman, 1996).

The NE-trending LFZ exists in the onshore–offshore transitional zone in shallow water, along which many large earthquakes occurred and the anomalous characteristics of gravity and geomagnetism are evident (Hao *et al*., 2002). It mainly dips southeast at a high angle (Cao *et al*., 2014). The crustal structure is greatly different on both sides of the LFZ, which suggests that the LFZ is the boundary between the normal continental crust of South China and the thinned continental crust of the northern SCS (Xia *et al*., 2010, 2014). A large number of cracked metamorphic granites can be observed in DI and Nanpeng Island, which may be due to the LFZ. The LFZ is extensively intersected with NW-trending faults. Previous studies inferred that the intersection of NW- and NE-trending local faults can control the occurrence of most small to moderate earthquakes, whereas the intersection of NW-trending faults and the LFZ might dominate the triggering of great earthquakes (Xu *et al*., 2006; Sun *et al*., 2012).

3 Data Acquisition

We conducted a large onshore–offshore seismic exploration experiment in the Pearl River Estuary from May to July in 2015. We used 50 oceanic bottom seismometers, 24-channel seismic cable, more than 100 portable seismometers on land, and seismic network in the coastal area as the receiving network. An airgun array with 6000 inch^3 in sea and high energy explosions on land were used as sources. A large number of 24-channel seismic and wide-angle seismic data were obtained in the experiment. The survey was carried out by *R/V Haidiao 6*. For navigation and shot timing, Global Positioning System was used. The ship speeds were 5.0–5.5 knots, and the array was fired at a time interval of 120 s, so the shot distance intervals ranged from 300 m to 330 m. More than 11000 shots were fired along ten NW–SE lines and three NE–SW lines (Fig.3). During the field operation, we encountered good weather conditions.

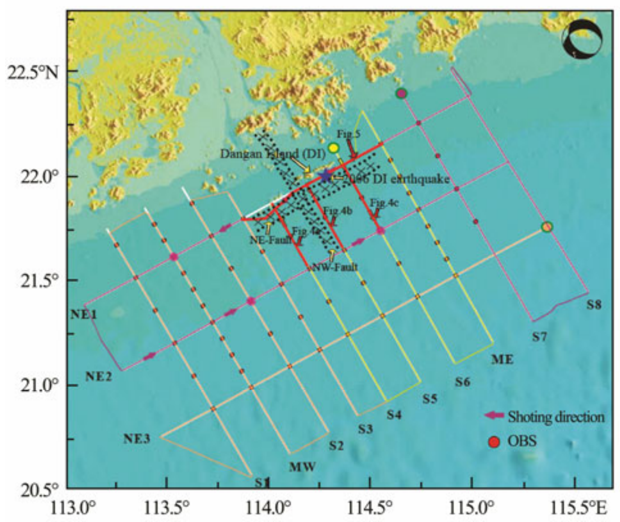

Fig.3 Location of 24-channel seismic and wide-angle seismic experiments in 2015. The red lines show the location of four single-channel seismic profiles used in this study. The blue star denotes the source of the 2006 Dangan Island earthquake. The dashed lines show the locations of NE and NW faults. The upper-right corner shows the focal mechanism of the 2006 DI earthquake.

In this study, we used three NW strike and one NE strike 24-channel seismic profiles near the DI sea area to investigate the locations and geometries of NE- and NW- trending faults. After a series of processing (Xia *et al.*, 2007), four 24-channel seismic sections were imaged (Figs.4 and 5). Amplitude spectra showed that the main seismic energy was in the frequency range of 3–20 Hz. Thus, the record sections were band-pass filtered from 3 Hz to 20 Hz to enhance the S/N ratio. We also used the published three-dimensional crustal structure in the DI area based on the 2004 onshore–offshore wide-angle data (Xia *et al.*, 2012) to analyze the structural variation in the source area of the 2006 DI earthquake. In addition, the 2006 M_L4.0 DI earthquake occurred at 19:53 in the evening of September 14, 2006 (Wong *et al.*, 2007), which induced the earth tremor felt widely in the Pearl River Estuary, including Hong Kong, Macau, Shenzhen, Zhuhai, Dongguan, Foshan, and Guangzhou. The epicenter was located at 21.99˚N, 114.23˚E over the sea near DI, and the focal depth was about 17 km (Wong *et al.*, 2007). The strike angles of the two nodal planes were ENE–WSW and NW–SE by determining the best fitting double-couple fault-plane solutions based on P-wave polarities recorded by the seismographic networks in Hong Kong, Guangdong, and Hainan (Wong *et al.*, 2007). Accordingly, we exploited the above integrated seismic data to study the sei-

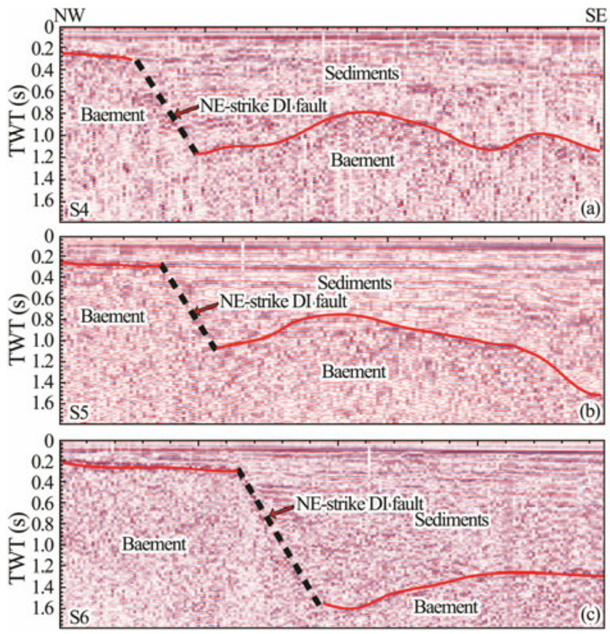

Fig.4 Single-channel seismic profiles along the NW–SE strike. The NE-strike Dangan Island (DI) fault is evident in the profiles (black dashed lines).

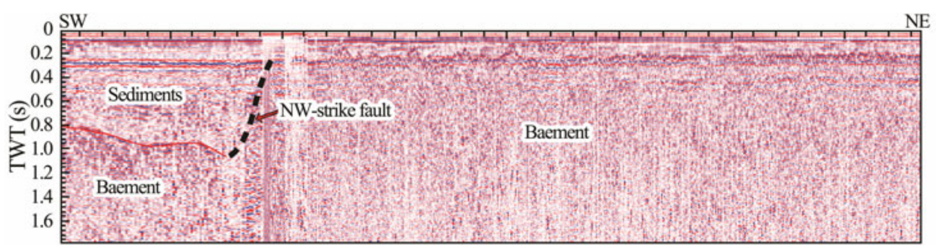

Fig.5 Single-channel seismic profiles along the SW-NE strike. The NW-strike fault is evident in the profile (black dashed line).

smogenic structure of the 2006 DI earthquake.

4 Results and Discussion

Two main sets of faults, namely, a dominant NE strike set and a subordinate NW strike set, were identified in and around Hong Kong (Lai and Langford, 1996; Fletcher, 1997), but how these different strike faults develop in the sea area remains unclear. Our present seismic profiles revealed the clear locations of NE and NW strike intersecting faults in the sea area (Figs.4 and 5). The NE-trending fault is located south of DI with water depth of 30–50 m, which is called the DI fault and considered part of the LFZ (Fig.4). This fault dips to the southeast direction and is parallel to the strike of DI. Figs.4a–4c show that the thickness of sedimentary strata sharply increases in the south of the fault, thereby suggesting the control effect of the DI fault on sedimentation. Lee *et al.* (1997) evaluated the movement potential of the major faults in and around Hong Kong, and they suggested that the NE-trending DI fault has the highest movement potential and capability to generate destructive earthquakes. The NW-trending fault was clearly observed in Fig.5 with the southwest dip, which intersected with the DI fault and cut DI into a number of separate peaks. The focal position of the 2006 DI earthquake was located near the intersection of the two sets of faults, indicating the important role of the intersecting faults with different strikes in the generation of an intraplate earthquake.

The 2006 DI earthquake was located at 21.99˚N, 114.23˚E with a focal depth of about 17 km, and its focal mechanism showed a strike-slip fault in either the ENE–WSW or NW–SE direction with a small normal faulting component (Wong *et al.*, 2007). To determine the deep features of the two sets of faults, we exhibited the P-wave velocity plan view at 17 km depth and two vertical cross-sections of the crustal structure that were approximately perpendicular to the strikes of intersecting faults (Fig.6) on the basis of the three-dimensional crustal model of Xia *et al.* (2012). Fig.6c reveals that a high-velocity (high-V) anomaly was detected in the Hong Kong region, whereas an obvious low-velocity (low-V) anomaly was imaged in the Pearl River Mouth; these results were consistent with surface geological features. We obtained about 3%–6% fast velocity anomaly with size of approximately 35 km× 20 km in the west of DI. This fast anomaly was a seismic and separated from the high-V anomaly beneath Hong Kong by a weak low-V zone denoting the NW-trending fault that is revealed in Fig.5. The region south of DI is characterized by distinct velocity anomaly that is anomalously slow in the upper crust but fast in the lower crust, which is in sharp contrast to the consistent positive velocity anomalies to the west of DI and in the Hong Kong region (Fig.6). The NE strike DI fault demarcates the transitional zone between the high-V region beneath Hong Kong and the distinct entity in the south of DI.

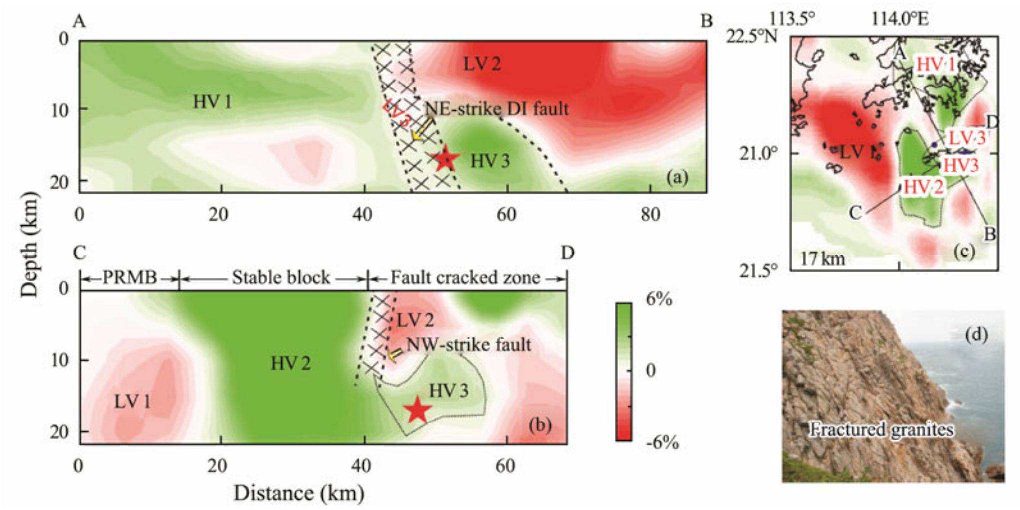

Fig.6 Seismic velocity structure along the NW–SE vertical section (a), SW–NE vertical section (b), and depth section at 17 km (c). Fractured granites extensively outcrop in DI (d). The NE-strike DI fault and NW-strike fault are shown in (a) and (b) with low to high-velocity transition, respectively. The red star in (a) and (b) is the location of the 2006 DI earthquake. The blue small and big stars denote the location of the 2006 and 1874 DI earthquakes according to the reference (Wong *et al.*, 2007), respectively.

Almost all earthquakes are distributed along the DI fault, and a good spatial correlation exists between seismicity and the distinct entity. These high-V bodies are separated and laterally offset from one another by NE and NW strike intersecting faults with relatively low-V features in the upper crust and then gradually form a united high-V body in the lower crust. Thus, the intersecting faults might be limited to the base of the lower crust. Previous studies implied that the intersecting fault zone might act as a localized stress concentrator and cause anomalous stress buildup in the vicinity, eventually resulting in the observed seismicity (Gangopadhyay and Talwani, 2005). Our present results showed that the 2006 DI earthquake occurred in the contact zone between the intersecting faults and the underlying high-V body in the south of DI, indicating that the underlying high-V body might be rigid and capable to store strain energy and release it as a brittle failure. The initiated rupture was propagated through the structural boundary between the intersecting faults and the underlying high-V body due to the relative mechanical weakness (Kato *et al*., 2005). However, the seismicity was only limited to the south of DI and the high-V region west of DI was a seismic, which indicated that the seismic activities might be suppressed by the stable high-V anomaly west of DI that functions as a seismic barrier (Aki, 1979). In addition, the intersecting fault zone was composed of minerals of low shear strength and highly cracked rocks according to field studies on DI (Fig.6d), which could become the path of fluids. Many studies have proven that fluids can lower the mechanical strength and frictional coefficient and play an important role in the nucleation and rupture of earthquakes (*e.g.*, Yamamoto *et al*., 2006; Reyners *et al*., 2007; Zhao *et al*., 2004b; Xia *et al*., 2008). Combined with the mechanisms of the high-V body as a strong and brittle asperity in the fault zone and the relatively low-V intersecting faults as a fluid path, we think that the complex of HV3 and intersecting faults in Fig.6 could be considered as the seismogenic structure.

In seismic risk studies, earthquakes along the DI fault are considered to have the greatest potential to give rise to strong earth tremors in Hong Kong (Chau *et al*., 2004). The present results demonstrated the possibility of a potential seismic hazard in the intersecting fault zone. Furthermore, our results indicated that the underlying high-V body in the south of DI reflected a strong and brittle asperity, which could further affect the dynamics of faults and alter stress of the fault zone, resulting in the rupture of an earthquake. In addition, fluids can pass through the cracked fault zone to affect the long-term structural and compositional evolution of the fault zone (Zhao *et al*., 2004b). These influences will enhance stress concentration in the seismogenic zone, leading to mechanical failure of a strong asperity (Zhao *et al*., 2004b) and possibly the nucleation of a large earthquake. Cochran *et al*. (2009) inferred that the fault damage zone is most likely weaker than the surrounding rock, facilitating the localization of regional strain. Strain localization of faults should be more responsive to relatively small stress changes (Cochran *et al*., 2009), thereby enhancing the potential of an earthquake-prone area in the intersecting fault zone. Thus, the contact zone between the intersecting fault zone and the underlying high-V body in the south of DI is the most potential earthquake-prone area near Hong Kong. This result is consistent with the present seismicity.

5 Conclusion

We used integrated seismic data to obtain the geometries from shallow to deep crust of different strike intersecting faults. The 2006 DI earthquake was found to occur adjacent to the intersection of NE and NW striking faults. A distinct entity with low velocity in the upper crust but high velocity in the lower crust was revealed in the south of DI. Both 1874 and 2006 DI earthquakes occurred along the edge of the distinct entity. Furthermore, the focal depth of the 2006 DI earthquake was located in the transitional zone of the low- and high-V bodies in the distinct entity. These results indicated that the intersecting faults might act as a localized stress concentrator and cause anomalous stress buildup in their vicinity, and the high-V body in the distinct entity could be rigid and capable of storing strain energy and releasing it as a brittle failure. Given the mechanisms of the high-V body as a strong and brittle asperity in the intersection of different strike faults and low-V faults as a fluid path, the contact zone between the intersecting faults and distinct entity may be the earthquake-prone area offshore Hong Kong.

Acknowledgements

The field work of this study was assisted by the Seismological Bureau of Guangdong Province and the captain and crew of *R/V Haidiao 6*. This work is jointly supported by the Strategic Priority Research Program of Chinese Academy of Sciences (No. XDA13010101), the National Natural Science Foundation of China (Nos. 91328 206, 41576041, 41506046), the Natural Science Foundation of Guangdong Province (No. 2017A030311015) and Special Project of Guangdong Province. Some figures in this paper were produced using Generic Mapping Tools (GMT) software written by Wessel and Smith.

References

Aki, K., 1979. Characterization of barriers on an earthquake fault. *Journal of Geophysical Research*, **84**: 6140-6148.

Assumpcao, M., Schimmel, M., Escalante, C., Barbosa, J. R., Rocha, M., and Barros, L. V., 2004. Intraplate seismicity in SE Brazil: Stress concentration in lithospheric thin spots. *Geophysical Journal International*, **159**: 390-399.

Barckhausen, U., Engels, M., Franke, D., Ladage, S., and Pubellier, M., 2014. Evolution of the South China Sea: Revised ages for breakup and seafloor spreading. *Marine and Petroleum Geology*, **58**: 599-611.

Briais, A., Patriat, P., and Tapponnier, P., 1993. Updated interpretation of magnetic anomalies and seafloor spreading stages in the South China Sea: Implications for the Tertiary tectonics of Southeast Asia. *Journal of Geophysical Research*, **98**: 6299-6328.

Campbell, S. D. G., and Sewell, R. J., 1997. Structural control and tectonic setting of Mesozoic volcanism in Hong Kong. *Journal of the Geological Society*, **154**: 1039-1052.

Cao, J., Sun, J., Xu, H., and Xia, S., 2014. Seismological features of the littoral fault zone in the Pearl River Estuary. *Chinese Journal of Geophysics*, **57** (2): 498-508 (in Chinese with English abstract).

Chandler, A. M., and Lam, N. T. K., 2002. Scenario predictions for potential near-field and far-field earthquakes affecting Hong Kong. *Soil Dynamics and Earthquake Engineering*, **22**: 29-46.

Chau, K. T., Wong, R. H. C., Wong, Y. L., Lai, K. W., Wang, L. X., Chan, Y. W., Wong, W. T., Guo, Y. S. H., Zhu, W., and Zheng, S. H., 2004. Three-dimensional surface cracking and faulting in Dangan Islands area, south of Hong Kong. *Proceedings of the Third International Conference on Continental Earthquakes*. Beijing, China, 12-14.

Cochran, E., Li, Y., Shearer, P., Barbot, S., Fialko, Y., and Vidale, J., 2009. Seismic and geodetic evidence for extensive, long-lived fault damage zones. *Geology*, **37** (4): 315-318.

Ding, Y. Z., and Lai, K. W., 1997. Neotectonic fault activity in Hong Kong: Evidence from seismic events and thermoluminescence dating of fault gouge. *Journal of the Geological Society*, **154**: 1001-1007.

Fletcher, C. J. N., 1997. The geology of Hong Kong. *Journal of the Geological Society*, **54**: 999-1000.

Gangopadhyay, A., and Talwani, P., 2003. Symptomatic features of intraplate earthquakes. *Seismological Research Letters*, **74**: 863-883.

Gao, J., Wu, S., McIntosh, K., Mi, L., Liu, Z., and Spence, G., 2016. Crustal structure and extension mode in the northwestern margin of the South China Sea. *Geochemistry*, *Geophysics*, *Geosystems*, **17** (6): 2143-2167.

Hao, T. Y., Liu, J. H., Song, H. B., and Xu, Y., 2002. Geophysical evidences of some important faults in South China and adjacent marginal seas region. *Progress of Geophysics*, **17** (1): 13-23 (in Chinese with English abstract).

Hole, J. A., Catchings, R. D., Clair, K. S., Rymer, M. J., Okaya, D. A., and Carney, B. J., 2001. Steep-dip seismic imaging of the shallow San Andreas Fault near Parkfield. *Science*, **294** (5546): 1513-1515.

Kato, A., Kurashimo, E., Hirata, N., Sakai, S., Iwasaki, T., and Kanazawa, T., 2005. Imaging the source region of the 2004 mid-Niigata prefecture earthquake and the evolution of a seismogenic thrust-related fold. *Geophysical Research Letters*, **32** (7): L07307.

Kato, A., Kurashimo, E., Igarashi, T., Sakai, S., Iidaka, T., Shinohara, M., Kanazawa, T., Yamada, T., Hirata, N., and Iwasaki, T., 2009. Reactivation of ancient rift systems triggers devastating intraplate earthquakes. *Geophysical Research Letters*, **36** (5): L05301.

Kenner, S., and Segall, P., 2000. A mechanical model for intraplate earthquakes: Application to the New Madrid seismic zone. *Science*, **289**: 2329-2332.

Koulakov, I., Bindi, D., Parolai, S., Grosser, H., and Milkereit, C., 2010. Distribution of seismic velocities and attenuation in the crust beneath the North Anatolian Fault (Turkey) from local earthquake tomography. *Bulletin of the Seismological Society of America*, **100**: 207-224.

Lai, K. W., and Langford, R. L., 1996. Spatial and temporal characteristics of major faults of Hong Kong. *Seismicity in Eastern Asia*, *Geological Society of Hong Kong Bulletin*, **5**: 72-84.

Lee, C. M., and Workman, D. R., 1996. Earthquakes in the South China region and their impact on Hong Kong. *Seismicity in Eastern Asia*, *Geological Society of Hong Kong Bulletin*, **5**: 92-103.

Lee, C., Hou, J., and Ye, H., 1997. The movement potential of the major faults in Hong Kong area. *Episodes*, **20**: 227-231.

Lester, R., Van Avendonk, H., McIntosh, K., Lavier, L., Liu, C., Wang, T., and Wu, F., 2014. Rifting and magmatism in the northeastern South China Sea from wide-angle tomography and seismic reflection imaging. *Journal of Geophysical Research*, **119** (3): 2305-2323.

Li, C. F., Li, J., Ding, W., Franke, D., Yao, Y., Shi, H., Pang, X., Cao, Y., Lin, J., Kulhanek, D. K., Williams, T., Bao, R., Briais, A., Brown, E. A., Chen, Y., Clift, P. D., Colwell, F. S., Dadd, K. A., Hernández-Almeida, I., Huang, X. L., Hyun, A., Jiang, T., Koppers, A. A. P., Li, Q., Liu, C., Liu, Q., Liu, Z., Nagai, R. H., Peleo-Alampay, A., Su, X., Sun, Z., Tejada, M. L., Trinh, H. S., Yeh, Y. C., Zhang, C., Zhang, F., Zhang, G., and Williams, T., 2015. Seismic stratigraphy of the central South China Sea Basin and implications for neotectonics. *Journal of Geophysical Research: Solid Earth*, **120** (3): 1377-1399.

Li, J., Ding, W., Wu, Z., Zhang, J., and Dong, C., 2012. The propagation of seafloor spreading in the southwestern subbasin, South China Sea. *Chinese Science Bulletin*, **57** (24): 3182-3191.

Liu, Y., 1981. *Analysis of Regional Faults Along the Coast of South China*. Seismological Press, Beijing, 1-120 (in Chinese).

Li, Z., and Li, X., 2007. Formation of the 1300-km-wide intracontinental orogen and postorogenic magmatic province in Mesozoic South China: A flat-slab subduction model. *Geology*, **35** (2): 179-182.

Liu, Z., Zhao, Y., Zhang, Y., Zhou, X., He, S., Xie, Y., Jiang, S., Wang, Q., Huang, Z., and Lin, J., 1997. A comprehensive study on Zhujiang River Mouth–Liyue Bank–Nansha Trough transect in the South China Sea. *Nanhai Studia Marina Sinica*, **12**: 1-24 (in Chinese with English abstract).

Megawati, K., 2007. Hybrid simulations of ground motions from local earthquakes affecting Hong Kong. *Bulletin of the Seismological Society of America*, **97**: 1293-1307.

Nissen, S. S., Hayes, D. E., Buhl, P., Diebold, J., Yao, B. C., Zeng, W. J., and Chen, Y. Q., 1995. Deep-penetrating seismic sounding across the northern margin of the South China Sea. *Journal of Geophysical Researchs*, **100** (B11): 22407-22433.

Pigott, J. D., and Ru, K., 1994. Basin superposition on the northern margin of the South China Sea. *Tectonophysics*, **235**: 27-50.

Qiu, X., Ye, S., Wu, S., Shi, X., Zhou, D., Xia, K., and Flueh, E., 2001. Crustal structure across the Xisha Trough, northwestern South China Sea. *Tectonophysics*, **341**: 179-193.

Reyners, M., D. Eberhart-Phillips, D., and Stuart, G., 2007. The role of fluids in lower-crustal earthquakes near continental rifts. *Nature*, **446**: 1075-1078.

Rocha, M. P., Azevedo, P. A., Marotta, G. S., Schimmel, M., and Fuck, R., 2016. Causes of intraplate seismicity in central Brazil from travel time seismic tomography. *Tectonophysics*, **680**: 1-7.

Schulte, S., and Mooney, W., 2005. An updated global earthquake catalogue for stable continental regions: Reassessing the correlation with ancient rifts. *Geophysical Journal Internation*, **161**: 707-721.

Shi, H., and Li, C., 2012. Mesozoic and early Cenozoic tectonic convergence-to-rifting transition prior to opening of the South China Sea. *International Geology Review*, **54** (15): 1801-1828.

Sibuet, J., Yeh, Y., and Lee, C., 2016. Geodynamics of the South China Sea. *Tectonophysics*, **692**: 98-119.

Sun, J., Xu, H., Zhan, W., and Cao, J., 2012. Activity and triggering mechanism of seismic belt along the northern South China Sea continental margin. *Journal of Tropical Oceanography*, **31** (3): 40-47 (in Chinese with English abstract).

Sykes, L., 1978. Intraplate seismicity, reactivation of preexisting zones of weakness, alkaline magmatism, and other tectonism postdating continental fragmentation. *Reviews of Geophysics and Space Physics*, **16** (4): 621-688.

Talwani, P., 1988. The intersection model for intraplate earthquakes. *Seismological Research Letters*, **59** (4): 305-310.

Talwani, P., and Rajendran, K., 1991. Some seismological and geometric features of intraplate earthquakes. *Tectonophysics*, **186**: 19-41.

Tapponnier, P., Peltzer, G., and Armijo, R., 1986. On the mechanics of the collision between India and Asia. *Geological Society*, *London*, *Special Publications*, **19** (1): 113-157.

Taylor, B., and Hayes, D. E., 1983. Origin and history of the South China Sea Basin. *The Tectonic and Geologic Evolution of Southeast Asian Seas and Islands*: *Part 2*, **27**: 23-56.

Wang, T. K., Chen, M., Lee, C., and Xia, K., 2006. Seismic imaging of the transitional crust across the northeastern margin of the South China Sea. *Tectonophysics*, **412**: 237-254.

Wittlinger, G., Tapponnier, P., Poupinet, G., Mei, J., Danian, S., Hequel, G., and Masson, F., 1998. Tomographic evidence for localized lithospheric shear along the Altyn Tagh Fault. *Science*, **282**: 74-76.

Wong, W., Chan, Y., Kang, Y., and Yang, X., 2007. Source Parameters of an M_L 4.0 Earthquake near Dangan Islands on 14.9.2006. *Asian–Pacific Network of Centers for Earthquake Engineering Research 2007 Meeting*. Hong Kong, China, 29-30.

Xia, S., Qiu, X., Tong, C., Xu, H., and Zhao, M., 2012. Three-dimensional tomographic model of the crust beneath the Hong Kong region. *Geology*, **40** (1): 59-62.

Xia, S., Qiu, X., Zhao, M., Ye, C., Chan, Y., Xu, H., and Wang, P., 2007. Data processing of onshore–offshore seismic experiment in Hongkong and Zhujiang River Delta region. *Journal of Tropical Oceanography*, **26** (1): 35-38 (in Chinese with English abstract).

Xia, S., Zhao, D., and Qiu, X., 2008. The 2007 Niigata earthquake: Effect of arc magma and fluids. *Physics of the Earth and Planetary Interiors*, **166**: 153-166.

Xia, S., Zhao, M., Qiu, X., Xu, H., and Shi, X., 2010. Crustal structure in an onshore–offshore transitional zone near Hong Kong, northern South China Sea. *Journal of Asian Earth Sciences*, **37**: 460-472.

Xu, H. L., Qiu, X. L., Zhao, M. H., Sun, J. L., and Zhu, J. J., 2006. Characteristics of the crustal structure and hypocentral tectonics in the epicentral area of Nan'ao earthquake (M7.5), the northeastern South China Sea. *Chinese Science Bulletin*, **51**: 95-106.

Yamamoto, Y., Hino, R., Nishino, M., Yamada, T., Kanazawa, T., Hashimoto, T., and Aoki, G., 2006. Three-dimensional seismic velocity structure around the focal area of the 1978 Miyagi–Oki earthquake. *Geophysical Research Letters*, **33**: L10308, DOI: 10.1029/2005GL025619.

Yan, P., Zhou, D., and Liu, Z., 2001. A crustal structure profile across the northern continental margin of the South China Sea. *Tectonophysics*, **338**: 1-21.

Zhang, Z., and Wang, Y., 2007. Crustal structure and contact relationship revealed from deep seismic sounding data in South China. *Physics of the Earth and Planetary Interiors*, **165**: 114-126.

Zhao, M., Qiu, X., Ye, C., Xia, K., Huang, C., Xie, J., and Wang, P., 2004a. Analysis on deep crustal structure along the onshore–offshore seismic profile across the Binhai (littoral) fault zone in northeastern South China Sea. *Chinese Journal of Geophysics*, **47** (5): 845-852 (in Chinese with English abstract).

Zhao, D., Tani, H., and Mishra, O. P., 2004b. Crustal heterogeneity in the 2000 western Tottori earthquake region: Effect of fluids from slab dehydration. *Physics of the Earth and Planetary Interiors*, **145**: 161-177.

Zoback, M., 1992. Stress field constraints on intraplate seismicity in eastern North America. *Journal of Geophysical Research*, **97**: 11761.

Zoback, M., 2010. Climate and intraplate shocks. *Nature*, **466**: 568-569.

(Edited by Chen Wenwen)